

Image Fusion and Fuzzy Clustering based Change Detection in SAR Images

Hire Gayatri Ashok
PG Student

R. C. Patel Institute of Technology, Shirpur,
Maharashtra, India

D. R. Patil

Assistant Professor

R. C. Patel Institute of Technology, Shirpur,
Maharashtra, India

ABSTRACT

Change detection in remote sensing images becomes more and more important for the last few decades, among them change detection in Synthetic Aperture Radar (SAR) images are having some more difficulties than optical ones due to the fact that SAR images suffer from the presence of the speckle noise. This paper presents unsupervised change detection in multi-temporal Synthetic Aperture Radar (SAR) images based on Image Fusion and Fuzzy Clustering algorithms. Image fusion technique is used to generate difference image by collecting information from Log ratio image and Mean ratio image. In order to intensify the information of changed regions and suppress the background information, Contourlet fusion rules are chosen to fuse the contourlet coefficients. For classifying changed and unchanged regions a reformulated FLICM (Fuzzy Local Information c-means) is proposed. This method reduces the effect of speckle noise because it is insensitive to noise. Experimental results, obtained on real multi-temporal SAR images by the Reformulated FLICM clustering algorithm exhibited low error than pre-existence.

General Terms

Synthetic Aperture Radar(SAR), difference image, image fusion, image change Detection algorithms

1. INTRODUCTION

Change detection is the method of detecting changes by analyzing images of the same scene taken at different times. In this context, one of the main uses of remote sensing is the detection of changes occurring after a natural or anthropic disaster. Change detection technique is used by many applications successfully, such as remote sensing [2], medical diagnosis [4], video surveillance [6], urban studies [7], forest monitoring [8] . One of the major data sources for remote sensing applications is synthetic aperture radar images [14], but there is one difficulties in synthetic aperture radar images than optical ones because of SAR images suffer from the presence of speckle noise. The main advantage of SAR images is SAR sensors which are independent of atmospheric and sunlight conditions.

Change detection may be done by supervised or unsupervised manner. In Supervised technique, training data set is required and in unsupervised technique, no requirement of training dataset. Therefore unsupervised technique is better than supervised technique.

In the literature, Unsupervised change detection in SAR images is carried out in to three steps: 1) Preprocessing of image; 2)producing the difference image; 3)analysis of the difference image. The aim of preprocessing is to increase the SNR of considering images by co-registration of images, geometric corrections, and noise reduction. In second step, difference image is generated by pixel by pixel comparison of co registered images. To producing the difference image, differencing (subtraction operator) and rationing (ratio operator) are well known techniques for remote sensing images. In differencing technique, changes are

calculated by subtracting the intensity values pixel by pixel between the considered couple of temporal images. In rationing technique, changes are obtained by applying a pixel by pixel ratio operator to the considered couple of temporal images. In case of SAR images, ratio operator is used because subtraction operator is nonrobust to calibration errors and it is not adapted to the statistics of SAR images [10] [11]. In addition, because of the multiplicative nature of speckles, the ratio image is usually expressed in a logarithmic or a mean scale. In the third step, change detection is usually carried out by applying a decision threshold to the histogram of the difference image. Several thresholding methods have been proposed in order to determine the threshold in an unsupervised manner, such as Otsu, the Kittler Illingworth minimum error thresholding algorithm, and the expectation maximization (EM) algorithm [15].

In general, from the literature it shows that the SAR image change detection performance is depend on the quality of the difference image and the accuracy of the classification method. In this paper, to address these two issues, we propose an unsupervised distribution-free SAR-image change detection approach. It is exclusive in the following two aspects: 1) producing difference images by fusing a mean-ratio image and a log-ratio image, and 2)improving the fuzzy local-information c-means (FLICM) clustering algorithm [34], which is noise insensitive, to identify the change areas in the difference image, without any distribution assumption. The fuzzy clustering methods that is, fuzzy c-means (FCM) algorithm is the method which is mostly used in image segmentation because it has robust characteristics for ambiguity and can retain much more information. By this method we can avoid the effect of speckle noise and to identify the changed areas in the difference image.

This paper organized into five sections, we discuss the main steps of the proposed approach and motivation in section II. Section III mainly focuses on the description of proposed method in details, and in section IV, presents the experimental results on the real multi-temporal SAR images will be described in detail to demonstrate the effectiveness of the proposed approach. Finally the last section V, presents our conclusion.

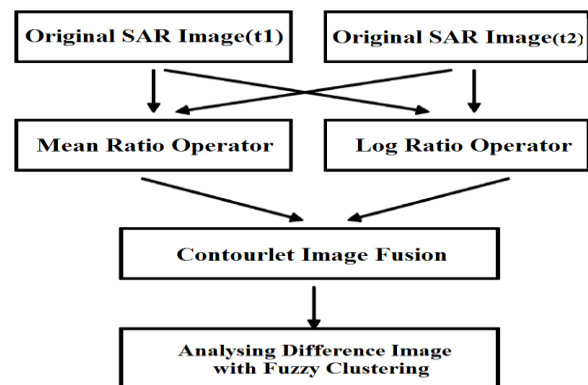


Fig. 1. Flow of the Proposed Change Detection Method

2. PROBLEM FORMULATION

To make the change detection problem more precise, let be an image sequence in which each image maps a pixel coordinate to an intensity or color. Let us consider the two coregistered intensity SAR images, $X_1 = [X_1(i, j), 1 \leq i \leq I, 1 \leq j \leq J]$ and $X_2 = [X_2(i, j), 1 \leq i \leq I; 1 \leq j \leq J]$ of size I.J, acquired over the same area at different times t_1 and t_2 . Our objective is aiming at producing a difference image that represents the change information between the two times; then, a binary classification is applied to produce a binary image corresponding to the two classes: change and unchanged. Unsupervised distribution-free change detection is made up of two main phases: 1) generate the difference image 2) automatic analysis of the fused image.

2.1 Motivation of Generating Difference Images using Image fusion

As mentioned in section I, due to the presence of speckle noise the ratio difference image is expressed in algorithmic or mean scale. The log ratio operator can be transformed the multiplicative speckle noise in an additive noise component. In [14], a ratio mean detector (RMD) is proposed by authors which is also robust to speckle noise. This detector assumes that a change in the scene will appear as a modification of the local mean value of the image. To detect the changes the results of both methods that is log ratio operator and ratio mean detector are effective. Although it has some disadvantages: The characteristic of logarithmic scale is to enhance the low intensity pixels and weakening the high intensity pixels in the areas; therefore, the distribution of two classes (changed and unchanged) could be made symmetrical. Due to the weakening in the areas of high intensity pixels, changed regions which are obtained by the log ratio image may not be able to reflect the real changed trends in the maximum extent. As for the RMD, the background (unchanged regions) of mean ratio image is quite uneven, for the ratio technique may highlight the differences in the low intensities of the temporal images. In general the basic idea of the best possible difference image is that unchanged pixels shows small values and changed areas shows larger values. It shows that the best possible difference image should restrain the background (unchanged areas) information and should enhance the information of changed regions. In this paper, to deal with this problem, image fusion technique is introduced in which the generation of difference image is done by using complementary information from the mean ratio image and the log ratio image. From the literature [10], [11], the information of changed regions reflected by the mean-ratio image is relatively in accordance with the real changed trends in multitemporal SAR images. Alternatively, the information of background obtained by the log ratio image is relatively smooth on account of the logarithmic transformation. From this we can conclude that individual difference images (i.e. log ratio image and mean ratio image) could obtain less information and the new difference image fused by mean ratio image and log ratio image could obtain better information content. The detailed description of this method will be presented in section 3.1.

2.2 Motivation of analyzing Difference Image Using Fuzzy Clustering

The main reason behind the processing of difference image is to differentiate the changed regions form unchanged regions. As described in section I, the KI algorithm and the EM algorithm are popular methods which are used to identify changed regions by applying a thresholding procedure to the histogram of the difference image. But this kind of methods have some disadvantages; that is it requires an accurate estimation of the decision threshold, and for classification of change and unchanged regions in the difference image they have to select proper

probability statistical model. This paper proposed a novel fuzzy c-means clustering algorithm to analyze the difference image which is insensitive to the probability statistics model of histogram. Precisely, this method incorporates the information about spatial context to the corresponding objective function for the purpose of reducing the effect of speckle noise. Detail description is given in the section 3

3. METHODOLOGY

This section describes the proposed change detection approach, which consist of two main steps: 1) Generate the difference image based on contourlet fusion, and 2) Detect changed areas in fused image using improved fuzzy c-means clustering algorithm.

3.1 Generate the Difference Image Using Contourlet Image Fusion

Image Fusion is the process of combining relevant information from two or more images into a single image. The resulting image will be more informative than any of the input images. Image fusion techniques can be classified on the basis of three levels: 1) Pixel Level 2) Feature Level 3) Decision making. From the past two decades, image fusion techniques mainly take place at the pixel level of the source images. For the pixel level image fusion multiscale transforms, such as the contourlets, curvelets, discrete wavelets transforms etc., has been used widely. The contourlet transform adopts non separable basis functions which make it capable of capturing the geometrical smoothness of the contour along any possible direction. Contourlet transform offers high degree of directionality. It has better performance in representing the image salient features such as edges, lines, curves, and contours than wavelet transforms. The two source images used for fusion are obtained from the mean-ratio operator and the log-ratio operator, respectively, which are given by [19].

$$X_m = 1 - \min(m_1/m_2, m_2/m_1) \quad (1)$$

$$X_1 = | \log X_1 / X_2 | = | \log X_1 - \log X_2 | \quad (2)$$

where m_1 and m_2 represent the local mean values of multitemporal SAR images X_1 and X_2 , respectively. The image fusion technique based on contourlet transform can be described as follows: Contourlet transform can be performed in two stages: 1) Transformation Stage 2) Decomposition Stage

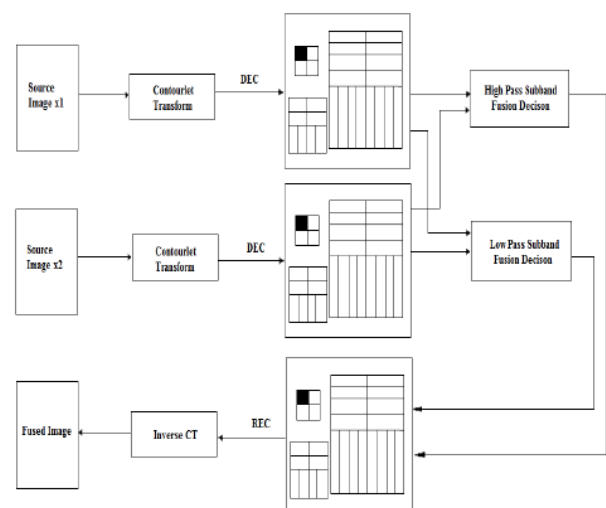


Fig. 2. Process of image fusion based on the contourlet Transform

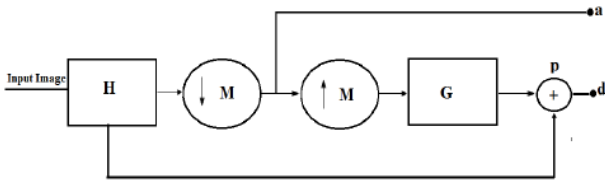


Fig. 3. Block diagram of construction of Laplacian pyramid Transform

3.1.1 Transformation Method

In the transformation stage, double filter bank is used for the decomposition of subbands. Double filter bank is composed of laplacian pyramid and directional filter bank, so it is also called pyramidal directional filter bank. For capturing the edge point, Laplacian pyramid filter is used. Directional Filter Bank is used to link the point discontinuities in the image [21]. In this method each input image undergone subband decomposition. That is in low frequency subbands and highfrequency subbands [21]. In the case of low frequency subband, the same process is repeated upto specified contourlet decomposition level. Above block diagram fig. 3 shows the laplacian pyramid decomposition. Here the input image is fed to a low pass analysis filter (H) and then down sampled to lowpass Subband. Then this image is up sampled and applied to a synthesis filter (G). Finally subtracting the output of the synthesis filter and input image we get highpass subbands [9]. The laplacian pyramid also allows high frequency bandpass image s into further decomposition, That is this bandpass images are passed through the directional filterbank. It captures directional information accurately. So in this tranformation stage, it decomposes the image into directional subbands at multiscale.

3.1.2 Decomposition Method

In this stage, decomposed subbands of transformation stage are fused by fusion rules. There are separate fusion rules for lowpass and highpass band. The coefficients in the lowpass subband represent the profile features of the source image. For this measurement local area energy contourlet domain is used. Then the selection and averaging modes are used to compute the final coefficients [21]. The local energy $E(x, y)$ is calculated by [9]

$$E(x, y) = \sum_m \sum_n a_j(x + m, y + n)^2 W_L(m, n) \quad (3)$$

Where (x, y) denotes the current contourlet coefficient, $W_L(m, n)$ is a template of size $3*3$ [9]. High frequency subbands which represent the salient features of the source image such as curves and lines. Average method is used for fusing the high frequency sub bands. It is defined as follows;

$$E_{jk}^F(x, y) = d_{jk}^A(x, y) + d_{jk}^B(x, y) \quad (4)$$

Where $E_{jk}^F(x, y)$ is the local energy, $d_{jk}^X(x, y)$ is the high frequency coefficient. Finally fused image is obtained from inverse contourlet decomposition method. The proposed method can provide fused image with better visual quality. And also the resultant fused image can preserve much information of edges and textures of SAR image. In the next section we describe novel fuzzy clustering algorithm for change detection in contourlet fused image.

3.2 Analysis of the Fused Image Using Improved Fuzzy c- means Clustering Algorithm.

The idea to process the difference image is to distinguish changed regions from unchanged regions. Also, clustering is the process for classifying objects or patterns in such away that samples of the same cluster are more similar to one another than samples

belonging to different clusters. Therefore, it can be considered that the problem of change detection can be viewed as a clustering problem where the key point is to divide the difference image data into two categories. Among the fuzzy clustering methods, the FCM algorithm is one of the most popular algorithm since it can retain more information from the original image and has robust characteristics for ambiguity's [20]. Here clustering is done to discriminate changed regions from unchanged regions. Recently, Krindis and Chatzis [34] have proposed a robust FLICM clustering algorithm to remedy the above shortcoming.

3.2.1 FLICM Clustering Algorithm

The characteristic of FLICM is the use of a fuzzy local similarity measure, which is aimed at guaranteeing noise in-sensitiveness and image detail preservation. In particular, a novel fuzzy factor $G(k_i)$ is introduced into the object function of FLICM to enhance the clustering performance. This fuzzy factor can be defined mathematically as follows:

$$G_{ki} = \sum_{\substack{j \in N_i \\ i \neq j}} \frac{1}{d_{ij} + 1} (1 - u_{kj})^m \|x_j - v_k\|^2 \quad (5)$$

where the i^{th} pixel is the center of the local window, the j^{th} pixel represents the neighboring pixels falling into the window around the i^{th} pixel, and d_{ij} is the spatial Euclidean distance between pixels i and j . v_k represents the prototype of the center of cluster k , and u_{kj} represents the fuzzy membership of the gray value j with respect to the k^{th} cluster. By using the definition of G_{ki} , the objective function of the FLICM can be defined in terms of

$$J_m = \sum_{i=1}^N \sum_{k=1}^c [u_{ki}^m \|x_i - v_k\|^2 + G_{ki}] \quad (6)$$

where v_k represents the prototype value of the k^{th} cluster and u_{ki} represents the fuzzy membership of the i^{th} pixel with respect to cluster k , N is the number of the data items, and c is the number of clusters. $\|x_i - v_k\|^2$ is the Euclidean distance between object and the cluster center v_k . In addition, the calculation of the membership partition matrix and the cluster centers is performed as follows:

$$u_{ki} = \frac{1}{\sum_{j=1}^c \left(\frac{\|x_i - v_k\|^2 + G_{ki}}{\|x_i - v_j\|^2 + G_{ji}} \right)^{\frac{1}{m-1}}} \quad (7)$$

$$v_k = \frac{\sum_{i=1}^N u_{ki}^m x_i}{\sum_{i=1}^N u_{ki}^m} \quad (8)$$

where the initial membership partition matrix is computed randomly. Finally, the FLICM algorithm is given as follows.

Step 1) Set the number c of the cluster prototypes, fuzzification parameter m and the stopping condition.

Step 2) Initialize randomly the fuzzy partition matrix.

Step 3) Set the loop counter $b = 0$.

Step 4) Compute cluster prototypes using (8).

Step 5) Calculate the fuzzy partition matrix using (7).

Step 6) If $\max \{U^b - U^{b+1}\} < \epsilon$ then stop, otherwise, set

$b = b + 1$ and go to step 4.

3.2.2 Reformulated FLICM

In the FLICM algorithm [34], the fuzzy factor G_{ki} cannot able to suppress influence of noisy pixels effectively. In order to overcome the shortcoming mentioned above, in this paper, the local coefficient of variation is adopted to replace the spatial distance. In addition, the local coefficient of variation C_u is defined by

$$C_u = \frac{\text{var}(x)}{(\bar{x})^2} \quad (9)$$

where $\text{var}(x)$ and \bar{x} are the intensity variance and the mean in a local window of the image, respectively. Due to the above mentioned disadvantage fuzzy factor G_{ki} is modified. New improved fuzzy factor is given by G

$$G'_{ki} = \begin{cases} \frac{\sum_{j \in n_i} \frac{1}{2 + \min((C_u^j/C_u)^2, (C_u/C_u^j)^2)}}{\times (1 - u_{kj})^m \|x_j - v_k\|^2} & \text{if } C_u \geq \bar{C}_u \\ \frac{\sum_{j \in n_i} \frac{1}{2 - \min((C_u^j/C_u)^2, (C_u/C_u^j)^2)}}{\times (1 - u_{kj})^m \|x_j - v_k\|^2} & \text{if } C_u < \bar{C}_u \end{cases} \quad (10)$$

where C_u is the local coefficient of variation of the central pixel, C_u^j represents the local coefficient of variation of neighboring pixels, C_u and \bar{C}_u is the mean value of that is located in a local window. As shown in (10), the reformulated factor G'_{ki} balances the membership value of the central pixel taking into account the local coefficient of variation, as well as the gray level of the neighboring pixels. If there is a distinct difference between the results of the local coefficient of variation that are obtained by the neighboring pixel and the central pixel, the weightings added of the neighboring pixel in G'_{ki} will be increased to suppress the influence of outlier; thereby, the reformulated FLICM, i.e., termed as RFLICM, is expected to be more robust to its pre-existence. Finally, by considering new fuzzy factor in FLICM, the RFLICM algorithm can be summarized as follows.

Step 1) Set the values of c , m & ϵ .

Step 2) Initialize randomly the fuzzy partition matrix & the loop counter $b=0$.

Step 3) Calculate the cluster prototypes (8).

Step 4) Compute the partitioning matrix (7).

$$v_k = \frac{1}{\sum_{i=1}^N u_{ki}^m}$$

Step 5) If $\max \{U^b - U^{b+1}\} < \epsilon$ then stop, otherwise, set

$b=b+1$ and go to step 3.

4. EXPERIMENTAL RESULTS

To validate our result now we will apply our algorithm to the Multitemporal SAR Images. For this purpose we have considered the Bern data set. This data set represents a section (301_301 pixels) of two SAR images acquired by the European Remote Sensing 2 satellite SAR sensor over an area near the city of Bern, Switzerland, in April and May 1999, respectively. Between the two dates, the River Aare flooded entirely parts of the cities of Thun and Bern and the airport of Bern. Therefore, the Aare Valley between Bern and Thun was selected as a test site for detecting flooded areas. The available ground truth (reference image), which was shown in Fig. 4(c), was created by integrating prior information with photo interpretation based on the input images Fig. 4(a) and 4(b). As mentioned in above sections the first task is to generate the difference image. Three difference images are generated by using Mean ratio, log ratio and the CWT fusion

method. Once we have the difference image, now we apply change detection algorithms to these images. Figure below shows the result obtained by applying FLICM algorithm. One can easily visualize, when the FLICM algorithm is applied to the difference image generated by CWT will give better result as compare to difference image generated by Mean ratio and Log ratio.

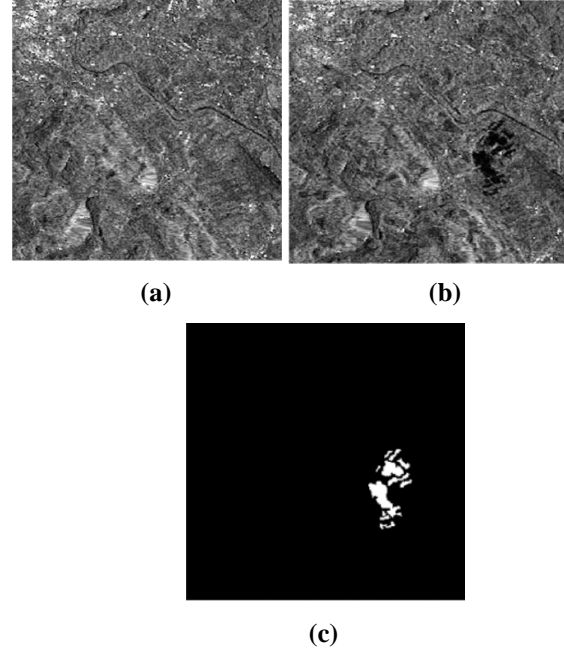


Fig. 4. Multitemporal images relating to the city of Bern used in the experiments. (a) Image acquired in April 1999 before the flooding. (b) image acquired in May 1999 after the flooding. (c) Ground truth.

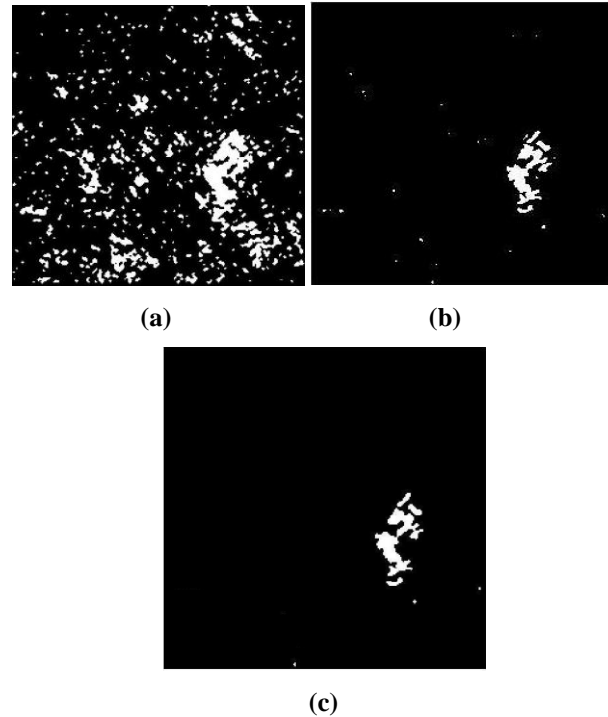


Fig. 5. Change detection results of the Bern data set based on the three difference images obtained by FLICM. (a) Based on the mean-ratio operator. (b) Based on the log-ratio operator. (c) Based on Contourlet fusion.

The quantitative analysis of change detection results is set as follow. These criteria are from [24]. First, we calculate the false negatives (FN, changed pixels that undetected). Second, we calculate the false positives (FP, unchanged pixels wrongly classified as changed). Third, we calculate the percentage correct classification (PCC). It is given by

$$PCC = \frac{TP + TN}{TP + FP + TN + FN} \quad (12)$$

Table 1 . Change detection result of the bern dataset Obtained by FLICM based on three difference images

Difference Image	FP	FN	PCC(%)
Mean Ratio	7550	1458	86.26
Log Ratio	2156	20	96.68
CWT	2137	21	96.71

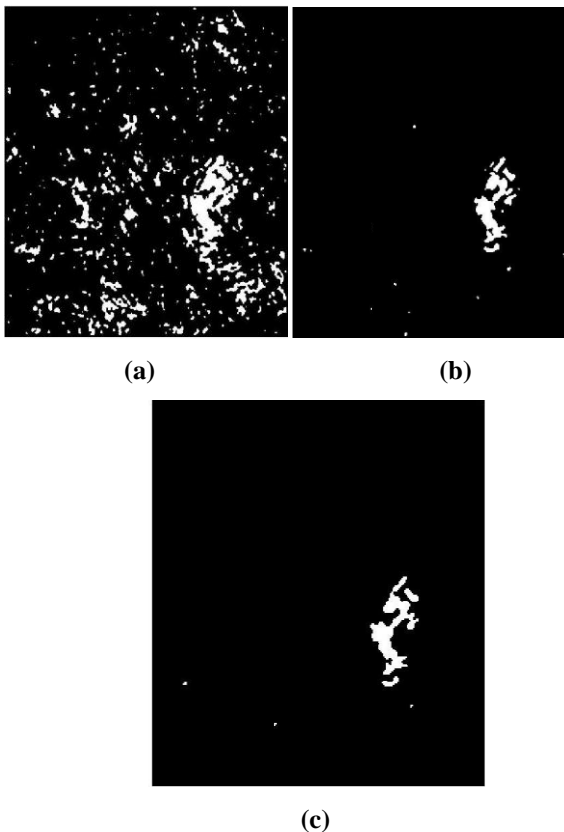


Fig. 6. Change detection results of the Bern data set based on the three difference images obtained by RFLICM. (a) Based on the mean-ratio operator. (b) Based on the log-ratio operator. (c) Based on Contourlet fusion.

Table 2. change detection result of the bern dataset Obtained by RFLICM based on three difference images

Difference Image	FP	FN	PCC(%)
Mean Ratio	6013	18	90.08
Log Ratio	2131	22	96.71
CWT	2097	22	96.77

5. CONCLUSION

In this paper, we have presented an unsupervised approach based on contourlet fusion and fuzzy clustering for change detection in SAR images. In order to restrain the unchanged areas and enhance the changed areas, fusion approach is used. Among the fusion methods, the limitations of wavelet transforms is capturing the geometry of image edges. So in this paper, contourlet transform is used because it can capture the intrinsic geometrical structure which is key in visual information. We show that, this method can provide fused image with better visual quality. In addition to that difference image produced in this method is better than that of fused difference image generated by Discrete wavelet Transform, Mean ratio and log ratio. The fused image obtained by Contourlet Transform can preserve much information of edges and textures of SAR images. The experiment results also show that the proposed contourlet fusion strategy can integrate the advantages of the log ratio operator and the mean-ratio operator and gain a better performance. The change detection results also shows that the RFLICM algorithm gives better result as compare to FLICM and its pre-existence.

6. REFERENCES

- [1] L. Bruzzone and D. F. Prieto, "An adaptive semiparametric and contextbased approach to unsupervised change detection in multi-temporal remote-sensing images", IEEE Trans. Image Process., vol. 11, no. 4, pp. 452-466, Apr. 2002.
- [2] Robin, L. Moisan, and S. Le Hegarat-Masclé, "An a-contrario approach for subpixel change detection in satellite imagery", IEEE Trans. Pattern Anal. Mach. Intell., vol. 32, no. 11, pp. 1977-1993, Nov. 2010.
- [3] M. Bosc, F. Heitz, J. P. Armspach, I. Namer, D. Gounot, and L. Rumbach, "Automatic change detection in multimodal serial MRI: Application to multiple sclerosis lesion evolution", Neuroimage, vol. 20, no. 2, pp. 643-656, Oct. 2003.
- [4] D. Rey, G. Subsol, H. Delingette, and N. Ayache, "Automatic detection and segmentation of evolving processes in 3-D medical images: Application to multiple sclerosis", Med. Image Anal., vol. 6, no. 2, pp. 163-179, Jun. 2002.
- [5] D. M. Tsai and S. C. Lai, "Independent component analysis-based background subtraction for indoor

- surveillance”, *IEEE Trans. Image Process.*, vol. 18, no. 1, pp. 158-167, Jan. 2009.
- [6] K.R., Merrill, and L., Jiajun. A Comparison of Four Algorithms for Change Detection in an Urban Environment. *Remote Sens. Environ.* 1998. 63 (2) 95-100.
- [7] T. Hame, I. Heiler, and J. S. Miguel-Ayanz, “An unsupervised change detection and recognition system for forestry”, *Int. J. Remote Sens.*, vol. 19, pp. 1079-1099, 1998.
- [8] S Rajkumar, S Kavitha, “Redundancy Discrete Wavelet Transform and Contourlet Transform for Multimodality Medical Image Fusion with Quantitative Analysis”, Third International Conference on Emerging Trends in Engineering and Technology, pp. 134-139.
- [9] A. Singh, “Digital change detection techniques using remotely sensed data”, *Int. J. Remote Sens.*, vol. 10, no. 6, pp. 989-1003, 1989.
- [10] E. J. M. Rignot and J. J. Van Zyl, “Change detection techniques for ERS-1 SAR data”, *IEEE Trans. Geosci. Remote Sens.*, vol. 31, no. 4, pp. 896-906, Jul. 1993.
- [11] Y. Bazi, L. Bruzzone, and F. Melgani, “An unsupervised approach based on the generalized Gaussian model to automatic change detection in multitemporal SAR images”, *IEEE Trans. Geosci. Remote Sens.*, vol. 43, no. 4, pp. 874-887, Apr. 2005.
- [12] J. Inglada and G. Mercier, “A new statistical similarity measure for change detection in multitemporal SAR images and its extension to multiscale change analysis”, *IEEE Trans. Geosci. Remote Sens.*, vol. 45, no. 5, pp. 1432-1445, May 2007.
- [13] W. Sezgin and B. Sankur, “A survey over image thresholding techniques and quantitative performance evaluation”, *J. Electron. Imag.*, vol. 13, no. 1, pp. 146-165, Jan. 2004.
- [14] Yaoguo Zheng, Xiangrong Zhang, Biao Hou and Ganchao Liu, “Using Combined Difference Image and k-Means Clustering for SAR Image Change Detection”, *Geoscience and Remote Sensing Letters.*, vol.11, no.3, pp.691-695, Aug. 2013.
- [15] Bruno Aiazzi, Luciano Alparone, Stefano Baronti, Andrea Garzelli, Claudia Zoppetti, “Nonparametric Change Detection in Multitemporal SAR Images Based on Mean-Shift Clustering”, *IEEE T. Geoscience and Remote Sensing*, vol.51, no.4 pp. 2022-2031, April. 2013.
- [16] Cyril Carincotte, Stphane Derrode, and Salah Bourennane, “Unsupervised Change Detection on SAR Images Using Fuzzy Hidden Markov Chains”, *IEEE Trans. Geosci. Remote Sens*, VOL. 44, NO. 2, Feb.2006.
- [17] Maoguo Gong, Zhiqiang Zhou and Jingjing Ma, “Change Detection in Synthetic Aperture Radar Images based on Image Fusion and Fuzzy Clustering.” *IEEE Trans. Image Process.*, vol. 21, no. 4, pp. 2141-2151, Apr. 2012.
- [18] J. C. Bezdek, *Pattern Recognition With Fuzzy Objective Function*. New York: Plenum, 1981.
- [19] L. Yang, B.L.Guo, W.Ni, “Multimodality Medical Image Fusion Based on Multiscale Geometric Analysis of Contourlet Transform”, Elsevier Science Publishers, vol. 72, pp. 203-211, December 2008.
- [20] J. Cihlar, T. J. Pultz, and A. L. Gray, “Change detection with synthetic aperture radar”, *Int. J. Remote Sens.*, vol. 13, pp. 401-414, 1992.
- [21] R. J. Dekker, “Speckle filtering in satellite SAR change detection imagery”, *Int. J. Remote Sens.*, vol. 19, pp. 1133-1146, 1998.
- [22] K. Grover and S. Quegan, “Quantitative estimation of tropical forest cover by SAR”, *IEEE Trans. Geosci. Remote Sens.*, vol. 37, no. 1, pp. 479-490, Jan. 1999.
- [23] C. Deledalle, L. Denis, and F. Tupin, “Iterative weighted maximum likelihood denoising with probabilistic patch-based weights”, *IEEE Trans. Image Process.*, vol. 18, no. 12, pp. 2661-2672, Dec. 2009.
- [24] R. O. Duda and P. E. Hart, “*Pattern Classification and Scene Analysis*”. Hoboken, NJ, USA: Wiley, 1973.
- [25] K. Fukunaga and L. D. Hostetler, “The estimation of the gradient of a density function, with applications in pattern recognition”, *IEEE Trans. Inf. Theory*, vol. IT-21, no. 1, pp. 32-40, Jan. 1975.
- [26] M. Fashing and C. Tomasi, “Mean shift is a bound optimization”, *IEEE Trans. Pattern Anal. Mach. Intell.*, vol. 27, no. 3, pp. 471-474, Mar. 2005.
- [27] Y. Cheng, “Mean shift, mode seeking, and clustering”, *IEEE Trans. Pattern Anal. Mach. Intell.*, vol. 17, no. 8, pp. 790-799, Aug. 1995.
- [28] D. Comaniciu and P. Meer, “Mean shift: A robust approach toward feature space analysis”, *IEEE Trans. Pattern Anal. Mach. Intell.*, vol. 24, no. 5, pp. 603-619, May 2002.
- [29] W. Skarbek, “Generalized Hilbert scan in image printing”, in *Theoretica Foundations of Computer Vision*, R. Klette and W. G. Kropetsch, Eds. Berlin, Germany: Akademik Verlag, 1992.
- [30] R. Dafner, D. Cohen-Or, and Y. Matias, “Context-based space filling curves”, *Comput. Graph. Forum*, vol. 19, no. 3, 2000.
- [31] J. Hungersfer and J. Wierum, “On the quality of partitions based on space-filling curves”, in *Int. Conf. Computational Science Amsterdam*, The Netherlands, vol. 21 no. 24, pp. 36-45, Apr. 2002.
- [32] S. Krinidis and V. Chatzis, “A robust fuzzy local information C-means clustering algorithm”, *IEEE Trans. Image Process.*, vol. 19, no. 5, pp. 1328-1337, May 2010.
- [33] J. D. Villasenor, D. R. Fatland, and L. D. Hinzman, “Change detection on Alaska north slope using repeat-pass ERS-1 SAR imagery”, *IEEE Trans. Geosci. Remote Sens.*, vol. 31, pp. 227-236, 1993.
- [34] L. G. Brown, “A survey of image registration techniques”, *ACM Comput. Surv.*, vol. 24, no. 4, 1992.
- [35] B. Zitov and J. Flusser, “Image registration methods: A survey”, *Image Vis. Comput.*, vol. 21, pp. 977-1000, 2003.
- [36] L. Ibez, W. Schroeder, L. Ng, and J. Cates, “The ITK Software Guide: The Insight Segmentation and Registration Toolkit”, 1.4 ed: Kitware, Inc., 2003.
- [37] A. Can, C. V. Stewart, B. Roysam, and H. L. Tanenbaum, “A feature based, robust, hierarchical algorithm for registering pairs of images of the curved human retina”, *IEEE Trans. Pattern Anal. Mach. Intell.*, vol. 24, no. 3, pp. 347-364, Mar. 2002.